Supramolecular Chemistry
Publication details, including instructions for authors and subscription information:
http://www.informaworld.com/smpp/title~content=t713649759

Precise patterning of photoactivatable glass coverslip for fluorescence observation of shape-controlled cells

Jun Nakanishi[a]; Yukiko Kikuchi[ab]; Yuki Tsujimura[c]; Hidekazu Nakayama[ad]; Shingo Kaneko[a]; Takahiro Shimizu[d]; Kazuo Yamaguchi[d]; Hideo Yokota[c]; Yasuhiko Yoshida[b]; Tohru Takarada[e]; Mizuo Maeda[e]; Yasuhiro Horiike[a]

[a] World Premier International (WPI) Research Center Initiative, International Center for Materials Nanoarchitectonics (MANA), National Institute for Materials Science (NIMS), Tsukuba, Japan [b] Graduate School of Engineering, Toyo University, Kawagoe, Japan [c] Bio-Research Infrastructure Construction Team, RIKEN, Wako, Japan [d] Department of Chemistry, Faculty of Science and Research Institute for Photofunctionalized Materials, Kanagawa University, Hiratsuka, Japan [e] Bioengineering Laboratory, RIKEN, Wako, Japan

Online publication date: 23 June 2010

To cite this Article Nakanishi, Jun , Kikuchi, Yukiko , Tsujimura, Yuki , Nakayama, Hidekazu , Kaneko, Shingo , Shimizu, Takahiro , Yamaguchi, Kazuo , Yokota, Hideo , Yoshida, Yasuhiko , Takarada, Tohru , Maeda, Mizuo and Horiike, Yasuhiro(2010) 'Precise patterning of photoactivatable glass coverslip for fluorescence observation of shape-controlled cells', Supramolecular Chemistry, 22: 7, 396 — 405

To link to this Article: DOI: 10.1080/10610278.2010.483735

URL: http://dx.doi.org/10.1080/10610278.2010.483735

Supramolecular Chemistry
Vol. 22, Nos. 7–8, July–August 2010, 396–405

Taylor & Francis
Taylor & Francis Group

Precise patterning of photoactivatable glass coverslip for fluorescence observation of shape-controlled cells

Jun Nakanishi[a]*, Yukiko Kikuchi[ab], Yuki Tsujimura[c], Hidekazu Nakayama[ad], Shingo Kaneko[a], Takahiro Shimizu[d], Kazuo Yamaguchi[d], Hideo Yokota[c], Yasuhiko Yoshida[b], Tohru Takarada[e], Mizuo Maeda[e] and Yasuhiro Horiike[a]

[a]*World Premier International (WPI) Research Center Initiative, International Center for Materials Nanoarchitectonics (MANA), National Institute for Materials Science (NIMS), Tsukuba, Japan;* [b]*Graduate School of Engineering, Toyo University, Kawagoe, Japan;* [c]*Bio-Research Infrastructure Construction Team, RIKEN, Wako, Japan;* [d]*Department of Chemistry, Faculty of Science and Research Institute for Photofunctionalized Materials, Kanagawa University, Hiratsuka, Japan;* [e]*Bioengineering Laboratory, RIKEN, Wako, Japan*

(*Received 29 January 2010; final version received 1 April 2010*)

The shape of cells is a key determinant of cellular fates and activities. In this study, we demonstrate a method for controlling the cellular shape on a chemically modified glass coverslip with micropatterned cell adhesiveness. The glass surface was chemically modified with an alkylsiloxane monolayer having a caged carboxyl group, where single-cell-sized hydrophilic islands with hydrophobic background were created by irradiating the substrate in contact with a photomask to produce the carboxyl group. Thus, the created surface hydrophilicity pattern was converted to a negative pattern of a protein-repellent amphiphilic polymer, Pluronic F108, according to its preferential adsorption to the hydrophobic surfaces. The following addition of a cell-adhesive protein, fibronectin, resulted in its selective adsorption to the irradiated regions. In this way, cell-adhesive islands were produced reproductively, and the cells formed a given shape on the islands. As examples of the cell-shape control, we seeded HeLa cells and NIH3T3 cells to an array of triangular spots, and fluorescently imaged the dynamic motions of cell protrusions extended from the periphery of the cells. The present method will not only be useful for studying the molecular mechanism of cell polarity formation, but also for studying other shape-related cellular events such as apoptosis, differentiation and migration.

Keywords: word; patterning; cell polarity; self-assembled monolayer; caged compound; fluorescence imaging

Introduction

The shape of cells is a key determinant of cellular fates and activities, such as survival/apoptosis (*1*, *2*), proliferation/differentiation (*3*), cell polarity (*4*), division (*5*, *6*) and migration (*7*). To elucidate the molecular mechanisms of their determination processes, it is straightforward to confine single cells in a given geometry and size, and examine the cellular behaviour in the microenvironments. Self-assembled monolayers (SAMs) with micropatterned cell adhesiveness are the most powerful tools for controlling cellular geometries and sizes. They can be easily formed by microcontact printing of alkanethiols on gold surfaces via a polydimethylsiloxane stamp (*8*), therefore many biological studies have been conducted on these substrates. However, the cells attached onto the gold substrates are not suited for microscopic observation, especially for fluorescence imaging, because fluorescence emitted from the cells is attenuated by absorption and scattering at the gold layers in the inverted objective set-up (*9*). In this aspect, it is more important to control cellular shapes on glass coverslips for high-speed and high-resolution imaging (*9–12*). We have recently reported a method for micropatterning cells on a glass coverslip whose surface was chemically modified with silane-coupling agents bearing a photocleavable 2-nitrobenzyl group (Figure 1(A)) (*13–15*). The substrate surface undergoes photochemical-reaction-driven hydrophilisation, which induces an exchange of surface-coated blocking agents (bovine serum albumin or Pluronic) with cell-adhesive proteins (e.g. fibronectin), eventually forming cellular patterns corresponding to the patterns of photoirradiation (Figure 1(B)). This substrate is considered suitable for fluorescence imaging because the thin silane monolayer does not perturb fluorescence observation. Moreover, the distinguished feature of this glass substrate from other normal micropatterned substrates is that it belongs to the so-called *dynamic substrates*, whose surface cell adhesiveness can be changed during cell cultivation by application of an external stimulus (*16–20*). Taking advantage of this feature, we have succeeded in the induction of migration and proliferation of selected single cells in a single cell array (*21*, *22*).

In our previous studies, the substrates were pattern-irradiated by the projection exposure of a photomask inserted at the field diaphragm of a fluorescence

*Corresponding author. Email: nakanishi.jun@nims.go.jp

ISSN 1061-0278 print/ISSN 1029-0478 online

DOI: 10.1080/10610278.2010.483735
http://www.informaworld.com

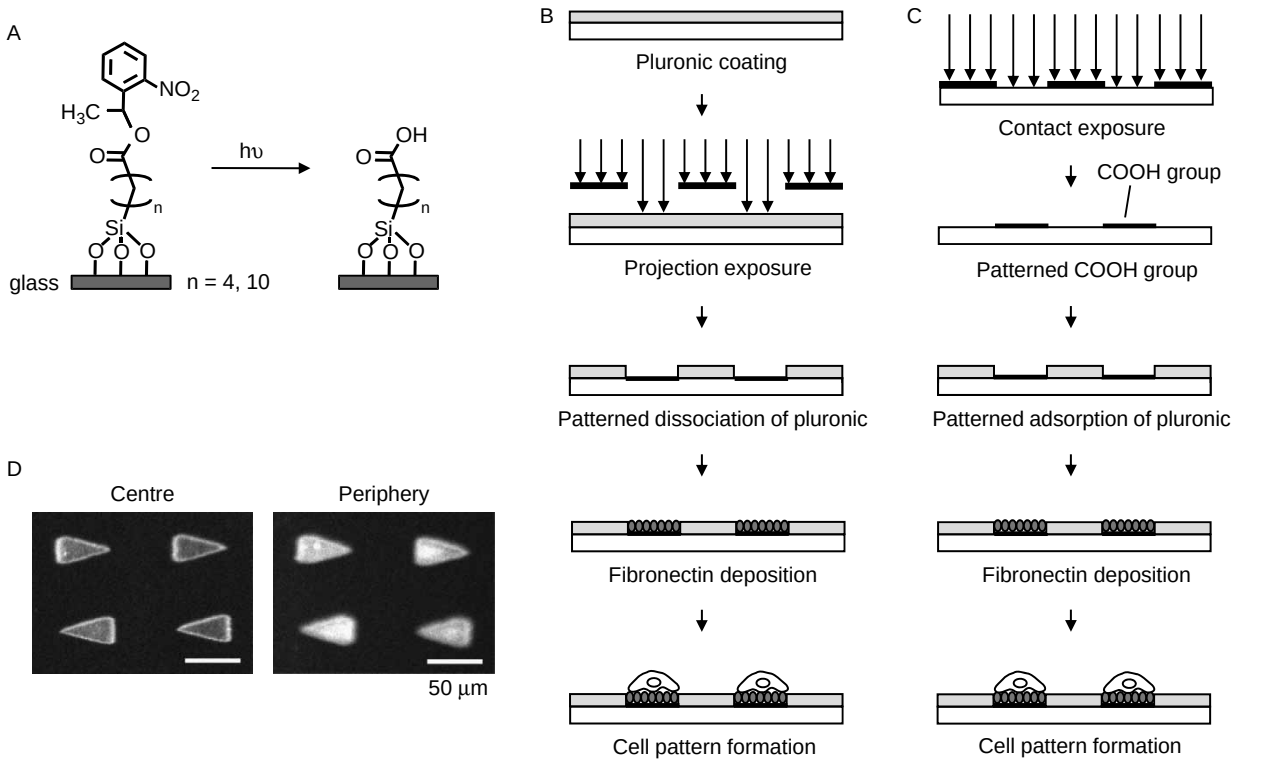

Figure 1. Cell patterning on photoactivatable glass substrates. (A) Photocleavage reaction of silane layers. (B) Surface patterning procedure used in our earlier studies. (C) Surface patterning procedure used in the present study. (D) Cell-adhesive fibronectin islands on photoactivatable glass, obtained according to the procedure shown in (B). Immunofluorescence images of the substrate at the central and peripheral portions of the visual field are shown.

microscope. This way of irradiation produced good projection at the central portion of the visual field, whereas it became blurred at the periphery causing an obscure boundary between non-cell-adhesive and cell-adhesive regions (Figure 1(D)). This propensity resulted in variation in the sizes and geometries of the cells, which was unfavourable for the precise study of the dependence of cellular activities on their microenvironments. In addition, it was also not favourable for analysing the cellular dynamic processes, such as migration and proliferation, induced by secondary irradiation because the initial cellular shape is one of the important factors that determine the direction and/or rate of motion. Therefore, we set our aim of the present study to improve the precision of the initial cellular patterns, which had remained unsolved in our previous works.

We changed the way of irradiation of the substrate from projection exposure to contact exposure, because the latter method is free from defocusing and has less possibility of diffraction. In addition, this irradiation method is more advantageous for mass production of patterned substrates than microscopic irradiation, which only illuminates a small portion (ca. 1 cm ϕ) of the substrate in our standard set-up.

According to the change in the exposure method, we changed the procedure for surface treatment. Pluronic was adsorbed onto the surface not before, but after the irradiation (Figure 1(C)) because surface drying caused detachment of Pluronic adsorbed onto the substrate surface. We examined the selectivity of Pluronic and fibronectin adsorption to the non-irradiated vs. irradiated regions on the substrates. We used two kinds of photoactivatable substrate with different lengths ($n = 4$ and 10) in the alkyl chain between trichlorosilyl and caged carboxyl groups (Figure 1(A)), because they were presumed to experience different hydrophobicity ranges during the photocleavage reaction. The modified procedure enabled reproducible production of cell-adhesive islands and fluorescence studies of the cells attached on the islands. These results clearly demonstrate that the present method can be used for the precise control of cellular shape on the photoactivatable glass substrate, which has been an urgent issue prior to the further investigation of dynamic cellular processes induced by secondary irradiation. In addition, it is important for the fluorescence observation of the shape-controlled cells as well as the cells in dynamic processes, such as migration and proliferation.

Experimental section

Reagents and instrumentation

Organic and inorganic solvents were purchased from Wako (Osaka, Japan) unless otherwise described. Pluoronic F108 was kindly supplied from BASF (Tokyo, Japan). 1-(2-Nitrophenyl)ethyl 5-trichlorosilylpentanoate and 1-(2-nitrophenyl)ethyl 11-trichlorosilylundecanoate were synthesised according to the procedures described previously (*13*, *21*). HeLa cells and NIH3T3 were obtained from RIKEN cell bank. HeLa cells were maintained in Dulbecco's modified Eagle's medium (DMEM; Sigma, St Louis, MO, USA) containing 10% heat-inactivated fetal bovine serum (FBS; Biowest, Miami, FL, USA), 100 U/ml penicillin and 100 μg/ml streptomycin at 37°C in 5% CO_2, and were subcultured every 2 or 3 days using 0.25% trypsin-EDTA (Invitrogen, Carlsbad, CA, USA). For culturing NIH3T3 cells, we used newborn calf serum (Invitrogen) instead of FBS.

All the images were captured with a cooled charge-coupled device camera Retiga-Exi (Q-Imaging, Burnaby, BC, Canada) under an IX-81 fluorescence microscope (Olympus, Tokyo, Japan) equipped with a mechanically automated filter changer MAC5000 (Ludl Electronic Products Ltd, Hawthorne, NY, USA), controlled by the MetaMorph image processing system (Molecular Devices, Downingtown, PA, USA). The contact angles were measured by using a contact angle meter, DropMaster 500 (Kyowa Interface Science, Saitama, Japan).

Preparation of photoactivatable substrates

Glass coverslips (30 mm^2 and 0.12–0.17 mm thick; Matsunami, Osaka, Japan) were cleaned in piranha solution [1:2 H_2O_2/H_2SO_4 (v/v), *Caution! Piranha is a vigorous oxidant and should be used with extreme caution*] for 1 h. After being cooled at room temperature, the glass substrates were rinsed with distilled water and then dried with a stream of dry nitrogen. The surface of the cleaned glass was modified either with 1-(2-nitrophenyl) ethyl 5-trichlorosilylpentanoate or 1-(2-nitrophenyl)ethyl 11-trichlorosilylundecanoate in dry benzene solution (1.4 mM) by refluxing for 1 h. The substrates were washed with methanol and dichloromethane, sonicated in dichloromethane for 15 min and dried with nitrogen.

Procedure for surface patterning

Photomasks were produced with a standard UV photolithographic technique. Briefly, a 63 mm^2 and 0.5 mm-thick quartz plate was sputter-coated with a Pt/Cr layer. The layer thickness was about 20 nm. This plate was then spin-coated with a positive-type electron-beam (EB) resist (OFPR-800; Tokyo Ohka Kogyo Co., Kawasaki, Japan). An equilateral triangular pattern of an aspect ratio of 1:2 was delineated on the resist by EB lithography (ELS-7500; Elionix, Tokyo, Japan). In a typical case, the photomask contained 86,400 triangular spots within an area of $30 \times 30\ mm^2$.

The photoactivatable substrate was placed on a homemade vacuum chamber that closely attached the substrate and the photomask. The substrate was irradiated with a mercury arc lamp (OPTICAL Modulex; Ushio, Tokyo, Japan) through a UV-transmitting filter (U330; HOYA, Tokyo, Japan) for a given energy. The power of UV light was measured by using a UIT-150 power meter equipped with UVD-S365 (Ushio). The substrate was sonicated in dichloromethane for 5 min and then in methanol for 5 min, and finally dried with a stream of dry nitrogen. The irradiated substrate was cut into small pieces and placed on a glass-bottom dish (MatTek, Ashland, MA, USA) and soaked in 1% Pluronic F108 in phosphate-buffered saline (PBS) overnight at room temperature. The substrate was washed with PBS several times, soaked in 25 μg/ml of fibronectin (BD Biosciences, Franklin Lakes, NJ, USA) for 5 min and washed again with PBS.

For cell patterning, $1–2 \times 10^5$ cells were seeded to the dish in serum-free minimum essential medium Eagle (MEM; Sigma), and were allowed to attach to the substrate at 37°C in a humidified atmosphere containing 5% CO_2. One hour after the seeding, the medium was changed to the serum-containing medium (DMEM-FBS or DMEM-NBCS).

Visualisation of surface pattern

To visualise Pluronic adsorbed onto the substrates, we used Pluronic labelled with Texas red. The fluorescent Pluronic was prepared according to the procedure described in the literature (*23*). Briefly, an aqueous solution of Pluronic F108 (5.4% in 0.1 M sodium bicarbonate, pH 9.0) and a DMSO solution of Texas Red C2-dichlorotriazine (Invitrogen) were mixed at a 1:1 (v/v) ratio at room temperature for 5 h in the dark. The mixed solution was applied to a NAP-10 column (GE, Buckinghamshire, UK) to remove unreacted Texas red. Thus, the obtained fluorescent Pluronic was mixed with unlabelled Pluronic at a 1:9 (v/v) ratio and used for fluorescence observation. Fluorescence images of the surface-adsorbed Pluronic were obtained by using the following set of barrier filters (Omega Optical, Brattleboro, VT, USA): 560AF75, 595DRLP and 645AF75.

Fibronectin adsorption was visualised by an immunofluorescence method. After fibronectin coating, the protein was fixed with 2% paraformaldehyde and reacted with 0.05 μg/ml rabbit anti-fibronectin IgG (Sigma), followed by a reaction with 4 μg/ml AlexaFluor 488-labelled goat anti-rabbit IgG. The fluorescence images of the substrates were obtained using the following set of barrier filters (Omega Optical): 485DF15, 505DRLPXR and 510ALP.

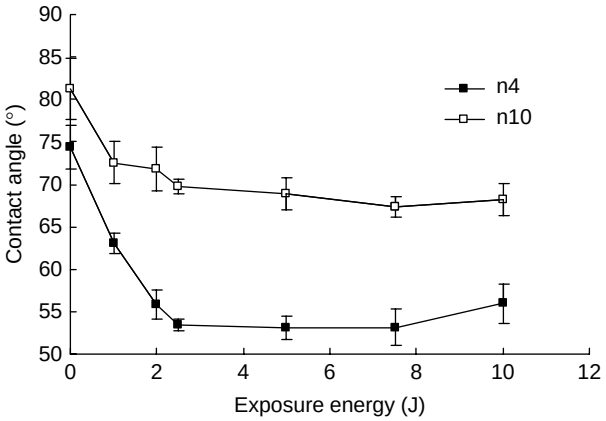

Figure 2. Contact angle profiles of the n4 and n10 substrates after irradiation of near-UV light for given energies.

In both the cases, fluorescence intensities were evaluated by averaging those of more than three different regions on the same substrate after subtracting the background fluorescence.

Fluorescence imaging of cell protrusions

NIH3T3 cells were transfected with Raichu-cdc42 by using lipofectamine 2000, and at 2 days after the transfection, the cells were seeded to the n4 substrate where 661 μm^2 triangular islands were transferred. The cell protrusions were visualised by monitoring the fluorescence of YFP band of Raichu-cdc42 by using UPLFLN40XO lens (Olympus) and the following set of barrier filters: FF500/24, FF520Di01 (Semrock, Rochester, NY, USA) and 542AF27 (Omega Optical).

Results and discussion

Surface wettability change upon photoirradiation

Photoactivatable glass substrates were prepared by surface modification of piranha-cleaned glass coverslips with one of the silane-coupling agents with different alkyl chain lengths ($n = 4$ and 10, Figure 1(A)). We hereafter refer to these substrates as 'n4 substrate' and 'n10 substrate', respectively. These substrates were presumed to exhibit a decrease in the contact angle in response to a near-UV irradiation by the photocleavage of the hydrophobic 2-nitrobenzyl group, as well as the exposure of the hydrophilic carboxyl group. Although we had already shown that the substrate surfaces become hydrophilic owing to irradiation in PBS (*13*, *21*), it is still important to investigate whether the same surface reaction takes place in air in the contact exposure mode, because we believe that surface hydrophilisation is the most essential driving force for changing the adsorbability of Pluronic and fibronectin.

The substrates were irradiated in air by near-UV light ($\lambda = 300–400$ nm) from a mercury arc lamp, and the photochemical reaction thereon was monitored by the water contact angle measurements (Figure 2). The contact angle of the n4 substrate was 75° before irradiation. It gradually decreased and reached a plateau (53°) by irradiation at 2.5 J (Figure 2, filled squares). On the other hand, the n10 substrate exhibited a similar tendency but with a smaller and more hydrophobic range (from 82° to 70°, Figure 2, open squares). The hydrophobic nature of the n10 substrate, when compared with the n4 substrate, was reasonable, considering the longer alkyl chain in the n10 substrate. Further increase in the irradiation energy caused

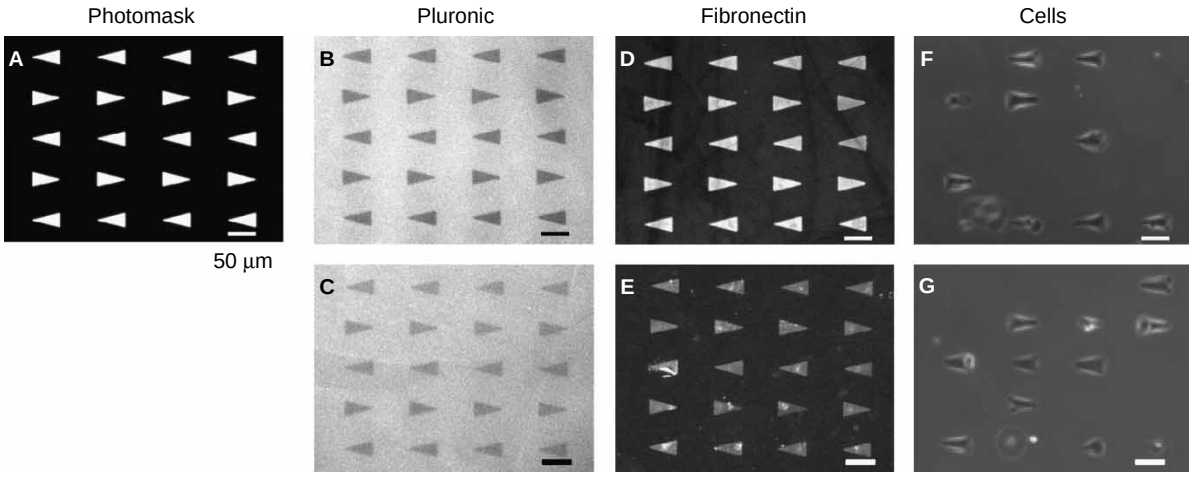

Figure 3. Process of formation of an array of cell-adhesive triangular islands. (A) A bright-field image of a photomask with an array of 661 μm^2 triangles. (B,C) Fluorescence images of Texas-red-labelled Pluronic adsorbed onto the n4 (B) and n10 (C) substrates after irradiation at 10 J in contact with the mask shown in (A). (D,E) Immunofluorescence images of the n4 (D) and n10 (E) substrates after depositing fibronectin onto the Pluronic-coated surfaces. Rabbit anti-fibronectin antibodies and Alexa 488-labelled anti-rabbit IgG were used. (F,G) Phase-contrast images of the n4 (F) and n10 (G) substrates at 3 h after seeding HeLa cells.

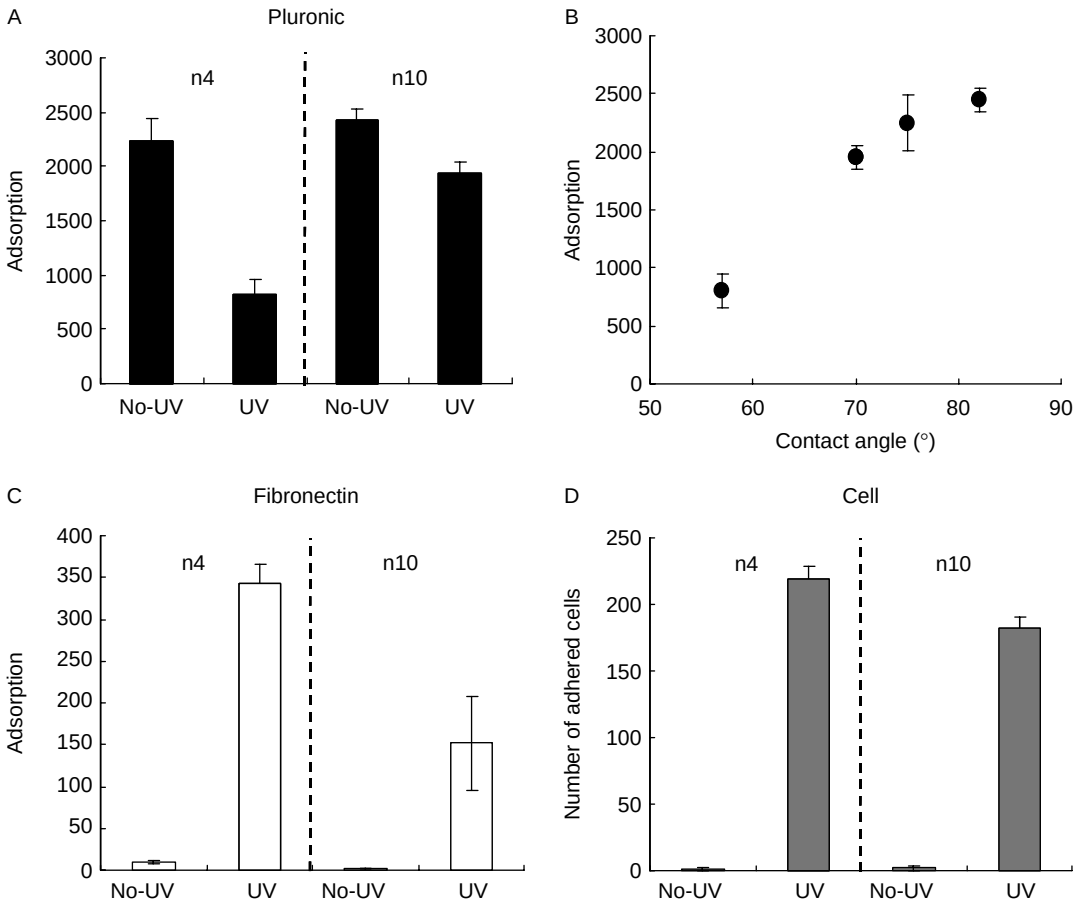

Figure 4. The amount of Pluronic and fibronectin adsorption and the number of cell adhesions onto non-irradiated and irradiated regions of the n4 and n10 substrates. (A) The amount of surface-adsorbed Pluronic determined by fluorescent Pluronic. (B) Effect of surface contact angles on Pluronic adsorption. The data in (A) were plotted against surface contact angle determined in Figure 2. (C) The amount of surface-adsorbed fibronectin onto the Pluronic-coated surfaces determined by an immunofluorescence method. (D) The number of HeLa cells adhered to the substrate surface after coating with Pluronic and fibronectin.

a slight increase in the contact angle in both the substrates (data not shown). However, such phenomena were not observed when the substrate was irradiated in PBS. The observed increases in the contact angle after prolonged irradiation in air were probably caused by some unexpected secondary reactions of nitrosoacetophenone, which was produced as a by-product of the photochemical reaction, because the compound was not able to diffuse from the surface within the photoirradiation time. On the basis of these results, we used irradiation at 10 J for all the subsequent experiments.

Generation of cell-adhesive islands according to photoirradiation

We next studied the process of the formation of cell-adhesive islands by following the procedure shown in Figure 1(C). The substrates were initially irradiated through a photomask having an array of triangular spots of 661 μm^2 (Figure 3(A)), and Pluronic and fibronectin were sequentially adsorbed onto the entire surface. The shape of the array spots was designed so as to polarise each single cell in the asymmetric geometry.

Texas-red-labelled Pluronic was used to visualise Pluronic adsorbed onto the substrate surface, and its adsorption amount was determined based on the brightness in the fluorescence microscopic images. We observed preferential adsorption of Pluronic onto the non-irradiated regions of the n4 and n10 substrates (Figure 3(B),(C)), which is in good agreement with the pattern of the photomask (Figure 3(A)). As can be seen from the better contrast in the fluorescence images, the difference in the amount of Pluronic adsorption between non-irradiated and irradiated regions was larger on the n4 substrate (Figure 4(A)). The selectivity of Pluronic adsorption (non-irradiated vs. irradiated) on the n4 substrate was 2.7, which was about twice as high as that of the n10 substrate (1.3). The results are consistent with the fact that the n4 substrate exhibited a greater change in the contact angle than the n10 substrate (*vide supra*). The dependence of Pluronic adsorption on

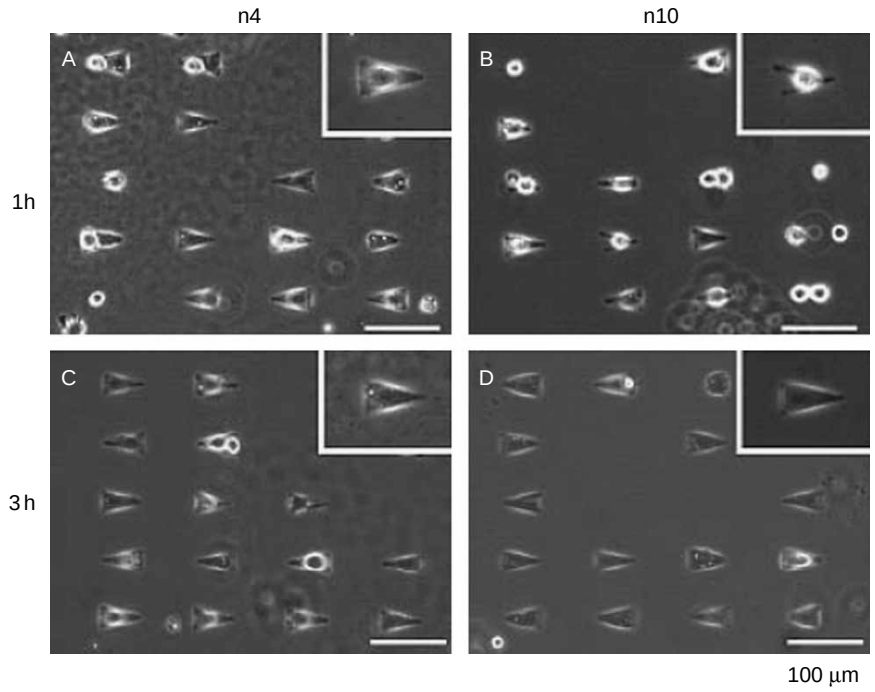

Figure 5. The process of cell spreading on triangular spots of 748 μm^2. (A–D) Phase-contrast images of HeLa cells adhered onto the n4 (A,C) and n10 (B,D) substrates at 1 h (A,B) and 3 h (C,D) after seeding. Magnified images of the representative cells are shown in the insets to clarify the degree of cell spreading.

surface hydrophobicity was more obvious when the amount of Pluronic adsorption was plotted against the surface contact angle of the substrates (Figure 4(B)). Within this wettability range, Pluronic was more strongly adsorbed onto the hydrophobic surfaces regardless of whether the substrates were irradiated or not. This tendency is in good agreement with the study by Chen and co-workers (*24*), in which the amount of Pluronic adsorption was examined on mixed SAMs of CH_3- and OH-terminated alkanethiols at various mixing ratios.

Next, the adsorption of fibronectin onto the Pluronic-treated substrates was examined by the immunofluorescence method using anti-fibronectin antibodies. Immunofluorescence images of the substrates (Figure 3(D),(E)) were opposite to the images of Pluronic (Figure 3(B),(C)), indicating that Pluronic adsorbed at the non-irradiated regions blocked fibronectin adsorption. When the amount of fibronectin adsorption was compared between the non-irradiated and irradiated regions, fibronectin showed highly preferential adsorption onto the irradiated substrates, and almost no adsorption onto the non-irradiated substrates (Figure 4(C)). This feature is important for the precise control of cellular shape in a given triangular geometry, because trace amount of fibronectin adsorbed to the surrounding will promote cells to foul beyond the boundary. It should also be emphasised that the selectivity of fibronectin adsorption was further enhanced from that of Pluronic. Considering the fact that more hydrophobic surfaces adsorb greater quantities of proteins (*25*), the adsorbability of fibronectin onto the Pluronic-treated substrates seemed to be basically determined by the pre-adsorbed amount of Pluronic rather than the affinity of the protein to bare substrate surfaces.

When HeLa cells were seeded to the substrate after the addition of fibronectin, the cells were selectively attached to the array spots. In Figure 3(F),(G), it can be observed that some of the array spots are not occupied by the cells. This is because we seeded the cells in rather low concentration in order to increase the occupancy of array spots by single cells. As discussed in detail in our previous paper (*15*), higher cell-seeding concentration increased the percentage of spots occupied by multiple cells. As the objective of this study was to control the shape of single cells, we seeded the cells in a lower concentration, compromising the net occupancy of the array spots.

The n4 substrate accommodated more single cells than the n10 substrate (Figure 4(D)). This result was reasonable considering the fact that the amount of adsorbed fibronectin was higher in the n4 substrate. In addition, the cells attached to the array spots on the n4 substrate spread immediately (Figure 5(A),(C)), whereas those on the n10 substrate were initially attached in rather round shapes and gradually spread over the irradiated spots to become triangles (Figure 5(B),(D)). The difference in the cell-spreading rate was also ascribed to the different amount of fibronectin. From these results, we concluded

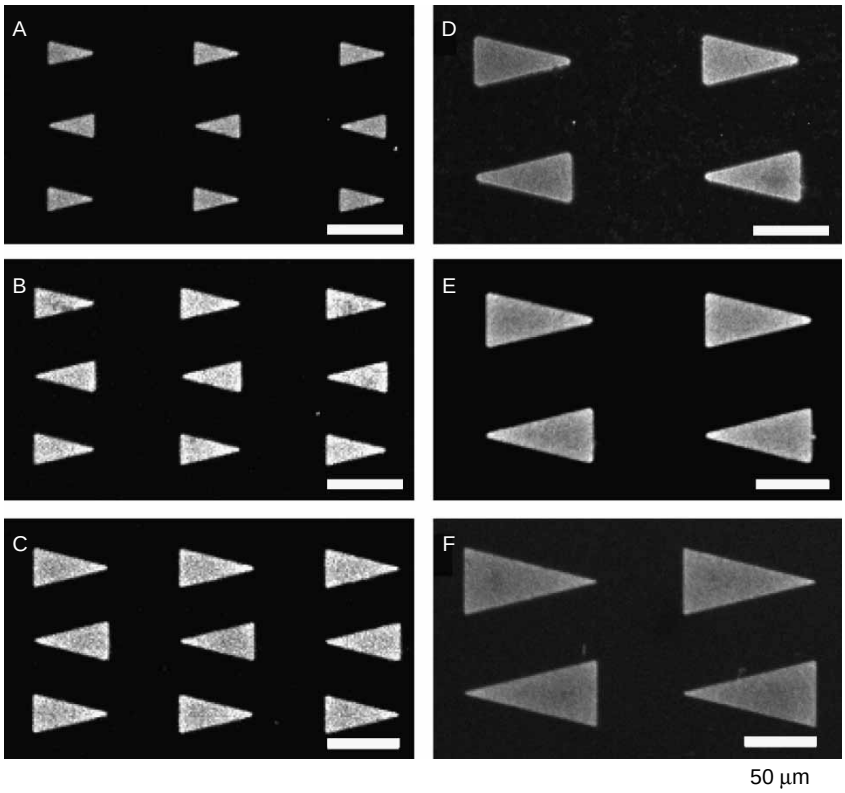

Figure 6. Immunofluorescence images of cell-adhesive triangular spots with various attaching areas. The n4 substrates were irradiated in contact with photomasks having (A) 224, (B) 400, (C) 661, (D) 942, (E) 1261 and (F) 2097 μm^2 triangular islands.

that the n4 substrate was more suitable than the n10 substrate in terms of the available number of single cells and rapid control of the cells in a given geometry.

Accuracy and precision of photopatterning

In order to evaluate the accuracy and precision of the present way of photopatterning on creating cell-adhesive spots, we compared the area of fibronectin islands with that of the original triangles drawn on the photomasks. The n4 substrate was irradiated in contact with a series of photomasks with triangular islands of different sizes (224, 400, 661, 942, 1261 and 2097 μm^2) with the same aspect ratio (ca. 2), and the cell-adhesive islands were analysed using anti-fibronectin antibodies.

The results are shown in Figure 6 and summarised in Table 1. The area of fibronectin islands was slightly larger than the triangles drawn in the photomask by 10–40% in size (Table 1). This enlargement in size was presumably because of the diffraction of light, even though the photomask and the substrates were closely attached. On the other hand, the relative standard deviation (RSD) of each spot was less than 3%; hence, we can conclude high precision of the cell-adhesive island formation in the contact exposure mode. Moreover, the shapes and sizes of the islands did not vary throughout the substrates. These results strongly support the notion that the contact exposure mode produces more precise cell-adhesive islands than the projection exposure mode that has been used in our previous studies (Figure 1(D)). Furthermore, with regard to the change in the surface treatment procedure, our photopatterning method has become more user-friendly to biological scientists. This is because we could pattern the cells by using a simple biochemical procedure, i.e. sequentially adding solutions of Pluronic and fibronectin to the substrate, when the substrate has been irradiated in large quantities in advance.

Fluorescence imaging of cell protrusions from triangular cells

Finally, we examined the dynamic motion of Cdc42 in NIH3T3 cells confined in a triangular shape based on the present method. Cdc42 is a member of the small GTPase superfamily (*26*). It is involved in the extension of thin, elongated protrusions called filopodia, whose extension is the key step during the early stage of the cell migration cycle. Therefore, the observation of the location and activity of Cdc42 in shape-controlled cells is important for understanding how cellular local and global geometries affect intracellular machineries to set off cell migration. NIH3T3 cells were transfected with Raichu-Cdc42 (*27*)

Table 1. Comparison of the area of triangles on mask and fibronectin islands.

Photomask (RSD)	224 ± 4 (1.8%)	400 ± 7 (1.8%)	661 ± 9 (1.3%)	942 ± 11 (1.2%)	1261 ± 11 (0.9%)	2097 ± 16 (0.8%)
Fibronectin (RSD)	317 ± 8 (2.5%)	523 ± 10 (1.9%)	748 ± 22 (2.9%)	1296 ± 23 (1.8%)	1535 ± 42 (2.7%)	2255 ± 64 (2.8%)
Enlargement[a]	1.4	1.3	1.1	1.4	1.2	1.1

Note: RSD, relative standard deviation.
[a]Enlargement = (area of fibronectin islands)/(area of triangles on mask).

which has two GFP mutants (YFP and CFP) at N- and C-termini. Although Raichu-Cdc42 reports the activity as well as the location of Cdc42, in the present study, we used this probe only for imaging the dynamic motions of cell protrusions.

Raichu-Cdc42 was distributed throughout the entire cells, but preferentially localised at the boundary between cell-adhesive islands and non-cell-adhesive surroundings. We could also observe the extension of widespread protrusions, called lamellipodia, from various parts of the triangle (Figure 7(A)), but the cells were confined alive within the spot for at least more than 7 h. To evaluate the dynamics of extension and regression of cell protrusions, the contour of the cells was traced every 10 s and superimposed (Figure 7(B)). The motion of the contour of the cells was active near the apical side (right side in the image) when compared with the basal side (left side in the image) of the triangle. The result was consistent with the study reported by Parker et al. (*28*), in which preferential extension of lamellipodia from sharp corners was reported. Furthermore, when focused on an active region near the apical side (square in Figure 7(A)), we were able to observe dynamic motions of filopodia (Figure 7(C)). However, visualisation of such thin structures in living cells could be difficult on micropatterned gold substrates, because the fluorescence signal is attenuated within the gold layers in the inverted objective set-up. To solve this drawback, earlier studies used fully or partially etched gold surfaces (*9*, *29*) or gold substrates in an upside-down configuration (*30*). However, attenuation of fluorescence signal should be minimised for high-speed and high-resolution images, and the procedure for sample preparation should be easy to operate. In addition, the substrate reported here has an advantage over the normal micropatterned glass substrate (*10–12*), because it not only allows controlling cells in a given shape, but also changing it by secondary irradiation (*21*). This feature is definitely useful for studying the spatio-temporal dynamics of intracellular biomolecules in response to the changes in the microenvironments of the cells.

Conclusions

In this study, a method for micropatterning of the photoactivatable glass substrate has been developed for the precise control of the initial cellular shape prior to their induction for migration and proliferation on the substrate. By using the contact exposure method for transferring patterns of photomasks to the substrate surface, reproducible production of cell-adhesive islands has been achieved. Thus, the formed cell-adhesive islands were used for fluorescence imaging of Cdc42 in NIH3T3 cells confined in a triangular shape, and the dynamic motions of filopodia as well as lamellipodia at the contour of the cells

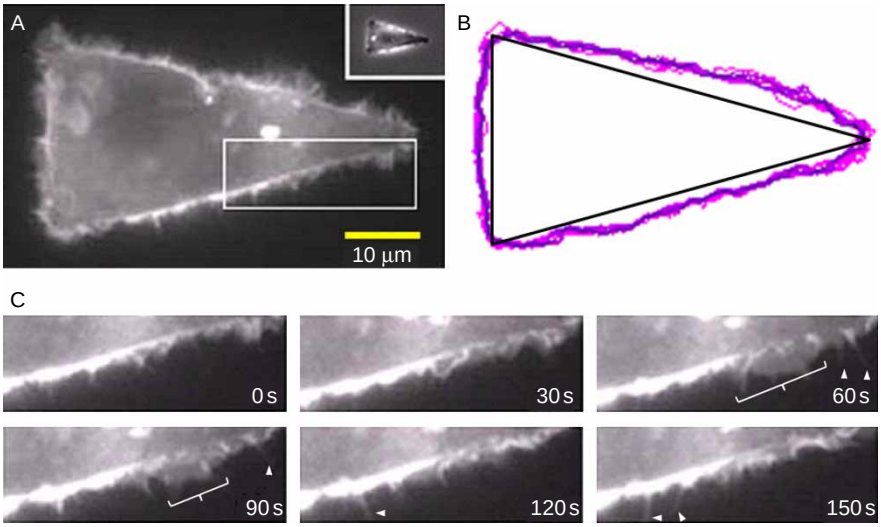

Figure 7. Dynamics of cell protrusions extended from the contour of an NIH3T3 cell confined in a triangular shape of 748 μm^2. (A) A fluorescence image of NIH3T3 cells expressing Raichu-Cdc42 monitored at the YFP band. A phase-contrast image of the same cell is shown in the inset. (B) A superimposition of the traces of the cellular outlines at every 10 s (pink). The outline at time 0 is drawn in blue line. The black triangle is the boundary of cell-adhesive and non-adhesive regions deduced from the cellular shape. (C) Extension and retardation of lamellipodia and filopodia within a square shown in (A) at given time points. Major lamellipodia and filopodia are indicated as braces and arrowheads (colour online).

were successfully observed. In contrast to conventional cell patterning techniques, the photoactivatable substrates reported here have distinguishing features that not only allow controlling the cellular shape, but also dynamically changing it by secondary irradiation. This feature has already been clearly demonstrated in our previous papers. It will be more interesting to fluorescently observe the signalling molecules in response to the change in the cellular shape by secondary irradiation, and it is currently under way.

Acknowledgements

This work was partially supported by a grant of Ecomolecular Science Research (to T.T. and M.M.) and Live Cell Modeling Project (to Y.T. and H.Y.) provided by RIKEN, and by the High-Tech Research Center Project from the Ministry of Education, Culture, Sports, Science, and Technology of Japan (to K.Y.). Y.K. also received support from a research fellowship of the Japan Society for the Promotion of Science (JSPS) for Young Scientists. We thank Dr Matsuda, Kyoto University and Dr Miyazaki, Osaka University for the expression vector of Raichu-Cdc42.

References

(1) Chen, C.S.; Mrksich, M.; Huang, S.; Whitesides, G.M.; Ingber, D.E. *Science* **1997**, *276*, 1425–1428.
(2) Nelson, C.M.; Chen, C.S. *FEBS Lett.* **2002**, *514*, 238–242.
(3) McBeath, R.; Pirone, D.M.; Celeste, M.N.; Bhadriraju, K.; Chen, C.S. *Dev. Cell.* **2004**, *6*, 483–495.
(4) Thery, M.; Racine, V.; Piel, M.; Pepin, A.; Dimitrov, A.; Chen, Y.; Sibarita, J.B.; Bornens, M. *Proc. Natl Acad. Sci. USA* **2006**, *103*, 19771–19776.
(5) Thery, M.; Racine, V.; Pepin, A.; Piel, M.; Chen, Y.; Sibarita, J.B.; Bornens, M. *Nat. Cell Biol.* **2005**, *7*, 947–953.
(6) Thery, M.; Jimenez-Dalmaroni, A.; Racine, V.; Bornens, M.; Julicher, F. *Nature* **2007**, *447*, 493–496.
(7) Jiang, X.Y.; Bruzewicz, D.A.; Wong, A.P.; Piel, M.; Whitesides, G.M. *Proc. Natl Acad. Sci. USA* **2005**, *102*, 975–978.
(8) Mrksich, M.; Dike, L.E.; Tien, J.; Ingber, D.E.; Whitesides, G.M. *Exp. Cell. Res.* **1997**, *235*, 305–313.
(9) Kandere-Grzybowska, K.; Campbell, C.; Komarova, Y.; Grzybowski, B.A.; Borisy, G.G. *Nat. Methods* **2005**, *2*, 739–741.
(10) Azioune, A.; Storch, M.; Bornens, M.; Thery, M.; Piel, M. *Lab Chip* **2009**, *9*, 1640–1642.
(11) Cuvelier, D.; Rossier, O.; Bassereau, P.; Nassoy, P. *Eur. Biophys. J. Biophys. Lett.* **2003**, *32*, 342–354.
(12) Thery, M.; Pepin, A.; Dressaire, E.; Chen, Y.; Bornens, M. *Cell Motil. Cytoskeleton* **2006**, *63*, 341–355.
(13) Nakanishi, J.; Kikuchi, Y.; Takarada, T.; Nakayama, H.; Yamaguchi, K.; Maeda, M. *J. Am. Chem. Soc.* **2004**, *126*, 16314–16315.
(14) Nakanishi, J.; Kikuchi, Y.; Takarada, T.; Nakayama, H.; Yamaguchi, K.; Maeda, M. *Anal. Chim. Acta* **2006**, *578*, 100–104.
(15) Kikuchi, Y.; Nakanishi, J.; Shimizu, T.; Nakayama, H.; Inoue, S.; Yamaguchi, K.; Iwai, H.; Yoshida, Y.; Horiike, Y.; Takarada, T.; Maeda, M. *Langmuir* **2008**, *24*, 13084–13095.
(16) Yamada, N.; Okano, T.; Sakai, H.; Karikusa, F.; Sawasaki, Y.; Sakurai, Y. *Makromol. Chem. Rapid Commun.* **1990**, *11*, 571–576.
(17) Yousaf, M.N.; Houseman, B.T.; Mrksich, M. *Proc. Natl Acad. Sci. USA* **2001**, *98*, 5992–5996.
(18) Jiang, X.Y.; Ferrigno, R.; Mrksich, M.; Whitesides, G.M. *J. Am. Chem. Soc.* **2003**, *125*, 2366–2367.

(19) Kaji, H.; Tsukidate, K.; Matsue, T.; Nishizawa, M. *J. Am. Chem. Soc.* **2004**, *126*, 15026–15027.
(20) Nakanishi, J.; Takarada, T.; Yamaguchi, K.; Maeda, M. *Anal. Sci.* **2008**, *24*, 67–72.
(21) Nakanishi, J.; Kikuchi, Y.; Inoue, S.; Yamaguchi, K.; Takarada, T.; Maeda, M. *J. Am. Chem. Soc.* **2007**, *129*, 6694–6695.
(22) Kikuchi, Y.; Nakanishi, J.; Nakayama, H.; Shimizu, T.; Yoshino, Y.; Yamaguchi, K.; Yoshida, Y.; Horiike, Y. *Chem. Lett.* **2008**, *37*, 1062–1063.
(23) Ahmed, F.; Alexandridis, P.; Neelamegham, S. *Langmuir* **2000**, *17*, 537–546.
(24) Tan, J.L.; Liu, W.; Nelson, C.M.; Raghavan, S.; Chen, C.S. *Tissue Eng.* **2004**, *10*, 865–872.
(25) Prime, K.L.; Whitesides, G.M. *Science* **1991**, *252*, 1164–1167.
(26) Hall, A. *Science* **1998**, *279*, 509–514.
(27) Kurokawa, K.; Matsuda, M. *Mol. Biol. Cell* **2005**, *16*, 4294–4303.
(28) Parker, K.K.; Brock, A.L.; Brangwynne, C.; Mannix, R.J.; Wang, N.; Ostuni, E.; Geisse, N.A.; Adams, J.C.; Whitesides, G.M.; Ingber, D.E. *FASEB J.* **2002**, *16*, 1195–1204.
(29) Lamb, B.M.; Westcott, N.P.; Yousaf, M.N. *Chembiochem* **2008**, *9*, 2220–2224.
(30) Hodgson, L.; Chan, E.W.L.; Hahn, K.M.; Yousaf, M.N. *J. Am. Chem. Soc.* **2007**, *129*, 9264–9265.